# On some structural characteristics of Fe-base shape memory alloys

A.-L. PARASCHIV[a], F. BORZA[b], N. LUPU[b], M.-G. SURU[a], N. M. LOHAN[a], B. PRICOP[a], I.-P. SPIRIDON[a], L.-G. BUJOREANU[a*]
[a]*Faculty of Materials Science and Engineering, The "Gheorghe Asachi" Technical University of Iaşi, Bd. D. Mangeron 61A, 700050 Iaşi, Romania*
[b]*National Institute of Research and Development for Technical Physics, Bd. D. Mangeron 47, 700050, Iaşi, Romania*

Two different types of Fe-base shape memory alloys (SMAs), obtained by different processing methods, were comparatively analyzed from the point of view of: (i) structural characterization, (ii) morphologic aspects and (iii) mechanical behaviour. For this purpose, heat treated specimens of Fe-9Cr-4Ni-0.33C and in Fe-28Ni-17Co-11.5 Al-2.5 Ta (mass. %) were produced and prepared for X-ray diffraction (XRD) and scanning electron microscopy (SEM) observations, which enabled to detect the presence of α' thermally induced martensite and γ austenite and to observed their respective morphologies. By means of micro-indentation tests, the variations of load vs. depth were recorded and the presence of pseudoelastic behaviour was confirmed, being ascribed to the presence of stable α' martensite. When α' martensite was stress-induced from γ austenite, being unstable upon unloading, a superelastic response was obtained, as was the case for Fe-28Ni-17Co-11.5 Al-2.5 Ta alloy.

(Received March 25, 2013; accepted July 11, 2013)

*Keywords*: Martensite, XRD, SEM, Micro-indentation, Pseudoelasticity, Reversible stress-induced transformation

## 1. Introduction

The term shape memory alloys (SMAs) comprise a group of metallic materials that demonstrate the ability to return to some previously defined shape or size when subjected to the appropriate thermal procedure [1]. Iron-based shape memory alloys have been extensively studied in the last years due to their good shape recovery properties compared to other materials [2]. Fe-based shape memory alloys can be divided into three groups based on their austenite and martensite structures: (i) those exhibiting a face-centred cubic (fcc) (austenite)–body-centred cubic tetragonal (bcc) (martensite) transformation, such as Fe-Pt base SMAs; (ii) those with a fcc (austenite)–hexagonal close-packed (hcp) (martensite) transformation, such as Fe-Mn base SMAs and (iii) those showing the fcc (austenite)– body-centred cubic tetragonal (bct) (martensite) transformation, such as Fe-Ni base SMAs [3].

Even if martensite has bcc structure in binary Fe-Ni alloys, due to very large thermal hysteresis (approx. 400 K), a certain tetragonality degree was observed, and as an effect of complex alloying, martensite structure became bct in some SMA systems [4]. Among alloying elements, the most common have been C [5]; Mn [6]; Nb [7]; Cr [8] and Co associated with Mo [9], Ti [10] or Al [11].

Besides shape memory, which is directly related to one way (1WE) and two way (2WE) shape memory effects, through a reversible martensitic transformation [12] Fe-Ni alloys are also characterized by superelasticity (SE). The superelastic response of a SMA is typically emphasized by the presence of a stress plateau on the unloading portion of a stress-strain curve, being caused by a reversible stress-induced martensitic transformation [13].

The observation of superelastic behaviour in Fe-base SMAs has been a constant preoccupation, ever since the 1980's, when these materials have started to be systematically characterized [14].

Unlike the beginning of 1990's, when 2 WE and SE were still considered as "unlikely" in Fe-based SMAs [15], at the end of the respective decade, a certain extent of SE was admitted to exist being favoured by low deformation rates and elevated test temperatures [16]. These encouraging results enabled the obtainment of a limited "pseudoelastically recovered strain" [17] without stress plateau during unloading [18], for Fe-28Mn-6Si-5Cr. On the other hand, in Fe-Ni based alloys experiencing $\gamma_{fcc}$ (austenite) - $\alpha'_{bcc}$ (martensite) transformation, large superelastic strains were predicted in Fe-Ni-Co-Ti, as an effect of high-temperature aging, causing the formation of $(CoNi)_3Ti$ disperse particles of γ′-phase. These particles have ordered atomic structure and are coherent with austenitic matrix which they reinforce through the increase of tetragonality degree [19]. The actual achievement of superelastic strains larger than 10 %, exceeding the customary thresholds reported in Ni-Ti base SMAs, was obtained in a Fe-28Ni-17Co-11.5Al-2.5Ta-0.05B with a strong {035}<100> recrystallization texture [11] which had the potential to trigger an expansion of SMA repertoire [20].

Aiming to replicate the "huge superelasticity" values (approx. 13 %) reported by Tanaka *et al.*, intense endeavours were spent for the development of Fe-Ni-Co-Al-Ta SMAs. Thus, aging heat treatment was optimized in such a way as to produce γ′-phase precipitates with an

average size of 5 nm, which however enabled superelastic strains lower than 4.5% [21]. With increasing aging time, at 923 K, up to 72 × 3.6 ks, γ′-phase precipitates changed their shape from 3-5 nm lamella to 10-15 nm granule [22].

The present paper aims to comparatively analyse the structures and related mechanical properties of two different Fe base alloys, Fe-Ni-Cr-C and Fe-Ni-Co-Al-Ta in aged state. The alloys were obtained by different processing routines, conventional casting and melt spinning, with the purpose to connect phase structure with pseudoelastic response.

## 2. Experimental details

An Fe-9Cr-4Ni-0.33C (mass. %) alloy was prepared by induction melting under Ar atmosphere, cast into cylindrical moulds and homogenized for 8 × 3.6 ks at 1300 K. $Fe_{40.95}Ni_{28}Co_{17}Al_{11.5}Ta_{2.5}B_{0.05}$ ribbons were been prepared by melt spinning technique and subjected to a complex heat treatment [23] comprising aging for 72× 3.6 ks at 873 K.

The specimens were embedded into could mounting and prepared for scanning electron microscopy (SEM) observations, performed by means of a SEM—VEGA II LSH TESCAN microscope, coupled with an EDX—QUANTAX QX2 ROENTEC detector as well as a JEOL JSM 6390 microscope. X-Ray diffraction measurements were performed using a D8 Advance - Bruker AxS GmbH diffractometer with Cu-$K_\alpha$ radiation, radiation intensity $I_e$=40mA and Voltage= 40KV. Micro-indentation tests were performed with a UMT-CETR universal tester at a maximum load of 13.5 N. Load-depth indentation curves were recorded, at a position precision of 1 × $10^{-7}$m, by means of the CETR data viewing software.

## 3. Results and discussion

The XRD pattern, recorded for aged Fe-9Cr-4Ni-0.33C (mass. %) alloy is shown in Fig. 1.

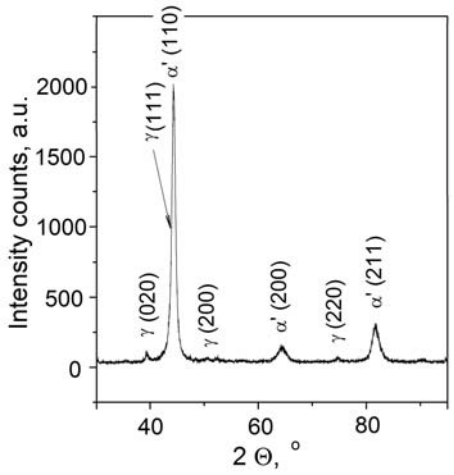


*Fig. 1. XRD pattern of aged Fe-9Cr-4Ni-0.33C (mass. %) alloy, illustrating the presence of α' thermally-induced martensite and γ retained austenite. The diffraction peaks of austenite and martensite overlap*

The main diffraction maximum can be ascribed to martensite as α'(110). The other maxima belonging to martensite are α'(200) and α'(211). In addition, there are three diffraction maxima which can be ascribed to retained austenite, as γ(020), γ(200) and γ(220) [18]. The main diffraction maximum of austenite, γ(111), overlaps on α'(110), the main peak of martensite but it is located to slightly lower 2θ angles [24].

In Fig. 2 the representative XRD pattern of aged $Fe_{40.95}Ni_{28}Co_{17}Al_{11.5}Ta_{2.5}B_{0.05}$ ribbons is illustrated.

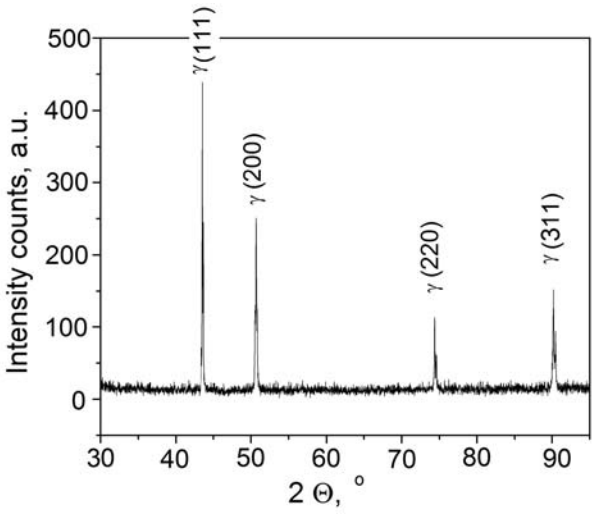


*Fig 2. XRD pattern of aged $Fe_{40.95}Ni_{28}Co_{17}Al_{11.5}Ta_{2.5}B_{0.05}$ ribbons, illustrating a fully austenitic structure*

It is noticeable that the entire structure is austenitic, which was expectable after 72× 3.6 ks at 873 K. This long-term holding was required by the possibility to preserve dendritic structure, in some Fe-Ni base alloys, even after 12× 3.6 ks maintaining at 923 K [25].

The morphological aspects of the structures of the two aged Fe base alloys under study were revealed by SEM observations coupled with EDX measurements. The representative SEM micrograph of aged Fe-9Cr-4Ni-0.33C alloy is illustrated in Fig.3.

The presence of stacks of thin martensite plates, in the aged condition of a Fe-Cr-Ni-C alloy, was also observed in heat treated Fe-7.4Mn-4.6Si-13.12Cr-6.35Ni-12.18Co-0.4Ti-0.03C [26]. On the other hand, the preservation of dendritic character of γ retained austenite represents a serious drawback of classical processing technologies based on casting. For this purpose alternative processing routines, such as powder metallurgy (PM) or melt spinning were developed.

PM was eventually associated with mechanical alloying (MA). Thus, stress induced formation of martensite in pre-strained [27] or mechanically cycled [28] hot rolled specimens, obtained from a PM-MA Fe-18Mn-3Si-7Cr-4Ni SMA, was reported. PM-MA alloys seemed unaffected by the small fraction of amorphous phase which partially crystallized during cyclic heating [29]. However, MA enabled the formation of α'-martensite in solution treated state, with detrimental effects on SM behaviour [30]. On the other hand, in the course of

developing a technology for obtaining porous Fe-Ni-Co-Ti powder alloys with thermoelastic martensite transformation, it was observed that both porosity and grain size have to be increased, in order to improve the properties [31].

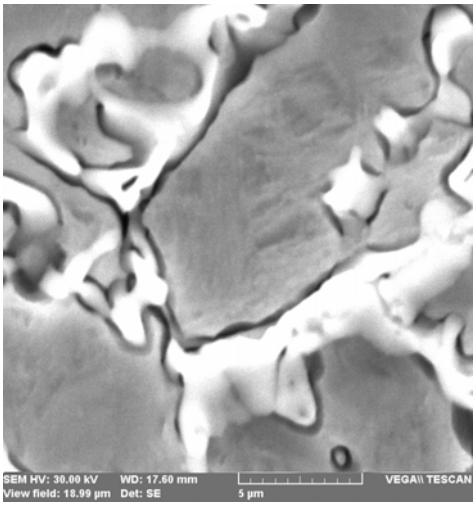


*Fig. 3. Typical SEM micrograph of aged Fe-9Cr-4Ni-0.33C, illustrating an area with very fine α' martensite bands surrounded by γ retained austenite with dendritic aspect.*

Melt spinning typical morphologic aspects of aged $Fe_{40.95}Ni_{28}Co_{17}Al_{11.5}Ta_{2.5}B_{0.05}$ ribbons are illustrated in Fig.4.

*Fig. 4. Typical SEM micrograph of aged ribbons of $Fe_{40.95}Ni_{28}Co_{17}Al_{11.5}Ta_{2.5}B_{0.05}$*

Here, again, some very fine platelets are noticeable, within some of γ-austenite grains, but they cannot be ascribed to martensite, as it will be shown later.

The surface relief of γ-phase was systematically observed by Benke *et al.*, through differential interference contrast imaging [32] being a peculiar morphologic aspect of the deformation at martensite transformation in Fe-Ni base SMAs [33]. It is noteworthy that, for thermally-induced martensite to form, liquid nitrogen cooling had to be applied, such as was the case of an Fe-Ni-Co-Ti-Cu alloy [34]. However, in order to obtain a superelastic response, it is not thermally-induced martensite but stress-induced martensite that has to be obtained from γ-austenite. Moreover, α' stress-induced martensite has to be unstable, such as to revert to γ-phase during isothermal unloading [13].

Chumlyakov *et al.* determined the main two conditions necessary to obtain a superelastic response in FeNiCoTi single crystals: (i) the critical temperature of the end of martensite reversion to austenite, $A_f$, should decrease below largest critical temperature where martensite formation is allowed by diffusion, $M_d$ and (ii) the critical stress for martensite stress-induced formation should be 5-7 times lower at $M_s$ (critical temperature for martensite formation on cooling) than at $M_d$, $\sigma_{cr}(M_d) \geq (5\text{-}7)\sigma_{cr}(M_s)$ [35].

On the other hand, in the specific case of FeNiCoAlTa single crystals, Chumlyakov *et al.* recently reported that, for superelasticity occurrence, ageing time at T=973K should be limited to 7 × 3.6 ks in such a way that γ'-phase precipitates not to exceed the size of 5 nm. When these γ' particles were uniformly distributed ordered in austenite matrix, with interparticle spacing comparable to their size, superelastic strains in tension as large as 14 % can be obtained. These values recommend superelastic Fe-Ni alloys as potential candidates for novel applications, such as power executive devices, meant to store large amounts of elastic energy [36].

The micro-indentation curves of the two alloys under study are shown in Fig.5

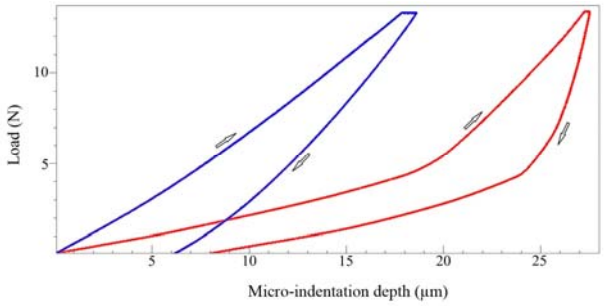


*Fig. 5. Micro-indentation curves, at a maximum load of 13.5 N, illustrating the increase of pseudoelastic response of the alloys under study: (a) Fe-9Cr-4Ni-0.33C revealing pseudoelasticity; (b) $Fe_{40.95}Ni_{28}Co_{17}Al_{11.5}Ta_{2.5}B_{0.05}$ revealing superelasticity*

Due to the pre-existence of α' thermally-induced martensite, aged Fe-9Cr-4Ni-0.33C alloy, experienced only a pseudoelastic response, during unloading, without any evidence of a stress plateau or even of a "pop-out event" [37]. Conversely, aged ribbons of $Fe_{40.95}Ni_{28}Co_{17}Al_{11.5}Ta_{2.5}B_{0.05}$, with fully austenitic structure, experienced a superelastic response, characterized by two distinctive stress segments on both loading and unloading portions. Fig.2 allows determining a proportion of approximately 47 % of crystallites oriented along $(111)_\gamma$, which could be an explanation of incomplete superelasticity observed in Fig.5 [38]. The superelastic character of the curve of $Fe_{40.95}Ni_{28}Co_{17}Al_{11.5}Ta_{2.5}B_{0.05}$ ribbons is much more pronounced in comparison to other results reported, for instance, at superelastic NiTi [39].

## 4. Conclusions

The pseudoelastic character, associated with α' martensite, was revealed by means of micro-indentation curves, as follows:

- No superelasticity was observed when α' thermally-induced martensite was already present in the structure of aged Fe-9Cr-4Ni-0.33C alloy.
- A superelastic recovery of micro-indentation depth larger than 70 % was obtained at aged melt spun $Fe_{40.95}Ni_{28}Co_{17}Al_{11.5}Ta_{2.5}B_{0.05}$ ribbons, being associated with the presence of γ-austenite which reversible transformed to α' stress-induced martensite.

**Acknowledgements**

This work was supported by UEFISCDI by the project PN.II-PT-PCCA-2011-3.1-0174, contract 144/ 2012.

## References

[1] D. E. Hodgson, M. H. Wu, R. J. Biermann, Shape memory alloys, ASM Handbook, Volume 2: Properties and Selection: Nonferrous Alloys and Special-Purpose Materials, ASM Handbook Committee, p. 897 (1990)
[2] T. Maki, Shape Memory Materials, K. Otsuka, C. M. Wayman (Eds.), Cambridge, University Press, p. 117 (1998)
[3] D Dunne, in Phase transformations in steels: Diffusionless transformations, high strength steels, modelling and advanced analytical techniques. Volume 2, E Pereloma and D V Edmonds (Eds), Woodhead Publishing, p. 83 (2012)
[4] H. Berns, W. Theisen, Ferrous Materials. Steel and Cast Iron, Springer-Verlag Berlin, p. 184 (2008)
[5] S. Kajiwara, T. Kikuchi, Acta Metall Mater **39**, 6, 1123 (1991)
[6] S. Kajiwara, Acta Metall, **32(**3), 407 (1984)
[7] Y. N. Koval, G. E. Monastirsky, Scripta Metall Mater, **28**, 41 (1993)
[8] T. Todaka, S. Teshima, M. Enokizono, J Mater Process Tech, **181(**1–3), 217 (2007)
[9] U. Sarı, E. Güler, T. Kırındı, M. Dikici, J Phys Chem Solids, **70**, 1226 (2009)
[10] N. Jost, Mat Sci Eng A, **273–275**, 649 (1999)
[11] Y. Tanaka, Y. Himuro, R. Kainuma, Y. Sutou, T. Omori, K. Ishida, Science, **327**, 1488 (2010),
[12] Y. X. Tong, B. Guo, F. Chen, B. Tian, L. Li, Y. F. Zheng, L. W. Ma, C. Y. Chung, Mat Sci Eng A, **550**, 434 (2012).
[13] T. W. Duerig, R., Zadno, in Engineering Aspects of Shape Memory Alloys, T. W. Duerig, K. N. Melton, D. Stöckel and C. M. Wayman, (Eds.), Butterworth-Heinemann, 369 (1990)
[14] A. Sato, E. Chisima, K. Soma, T. Mori, Acta Metall **30**, 1177 (1982)
[15] J. H. Yang, H. Chen, C. M. Wayman, Metall Trans A, **23**, 1431 (1992)
[16] N. Bergeon, G. Guenin, C. Esnouf, Mat Sci Eng A, **242**, 87 (1998)
[17] O. Matsamura, T. Sumi, N. Tamura, K. Sakao, T. Furukawa, H. Otsuka, Mat Sci Eng A, **279**, 201 (2000)
[18] T. Sawaguchi, T. Kikuchi, S. Kajiwara, Smart Mater Struct **14**, 317 (2005)
[19] Yu. I. Chumlyakov, I. V. Kireeva, E. Yu. Panchenko, V. B. Aksenov, V. A. Kirillov, A. V. Ovsyannikov, E. G. Zakharova, and H. Sehitogly, Russ Phys J, **46(**8), 811 (2003)
[20] J. Ma, I. Karaman, Science, **327**, 1468 (2010)
[21] J. Ma, B. Kockar, A. Evirgen, I. Karaman, Z.P. Luo, Y.I. Chumlyakov, Acta Mater **60,** 2186 (2012)
[22] Yonghong Geng,Mingjiang Jin, Wenjing Ren, Weimin Zhang, Xuejun Jin, J Alloy Compd, doi:10.1016/j.jallcom.2012.03.033 (2012)
[23] F. Borza, A. L. Paraschiv, L. G. Bujoreanu, N. Lupu, ICPAM-9, 42 (2012)
[24] T. Volkmann, W. Löser, D. M. Herlach, Metall Mater Trans A, **28A**, 461 (1997)
[25] S. Buyukakkas, H. Aktas, S. Akturk, J Univ Sci Technol B, **14(**4), 327 (2007)
[26] K. A. Käfer, H. H. Bernardi, L. K. F. Naito, N. Batista de Lima, J. Otubo, Materials Science Forum, **738-739**, 496 (2013)
[27] L. G. Bujoreanu, S. Stanciu, B. Özkal, R. I. Comăneci, M. Meyer, ESOMAT 2009, 05003 (2009)
[28] B. Pricop, U. Söyler, R. I. Comăneci, B. Özkal, L. G. Bujoreanu, Physics Procedia **10**, 125 (2010)
[29] B. Pricop, U. Söyler, N. M. Lohan, B. Özkal, D. Chicet, A. David, L.-G. Bujoreanu, Optoelectron Adv. Mater – Rapid Commun **5(**5), 555 (2011)
[30] B. Pricop, U. Söyler, B. Özkal, N. M. Lohan, A. L. Paraschiv, M. G. Suru, L. G. Bujoreanu, Materials Science Forum, **738-739**, 237 (2013)
[31] O. M. Shevchenko, G. V. Gavrilyuk, V. V. Kokorin, V. A. Chernenko, Powder Metall Met C **36(**1-2), 71 (1997)
[32] M. Benke, V. Mertinger, F. Tranta, Materials Science Forum, **738-739**, 257 (2013)
[33] V. Gundyrev, V. Zel'dovich, Materials Science Forum, **738-739**, 20 (2013)
[34] A. N. Titenko, L. D. Demchenko, J Mater Eng Pefform doi: 10.1007/s11665-012-0406-x (2012)
[35] Yu. I. Chumlyakov, I. V. Kireeva, E. Yu. Panchenko, E. G. Zakharova, V. A. Kirillov, S. P. Efimenko, H. Sehitoglu, Dokl Phys, **49(**1), 47 (2004)
[36] Yu Chumlyakov, I. Kireeva, I. Kretinina, V. Kirillov, O. Kuc, I. Karaman, H. Maier, E. Cesari, ESOMAT 2012, 73 (2012)
[37] C. Maletta, F. Furgiuele, E. Sgambitterra, M. Callisti, B. G. Mellor, R. J.K. Wood, Frattura ed Integrità Strutturale, **21**, 5 (2012)
[38] Yu. I. Chumlyakov, I. V. Kireeva, I. Karaman, E. Yu. Panchenko, E. G. Zakharova, A. V. Tverskov, A. V. Ovsyannikov, K. M. Nazarov, V. A. Kirillov, Russ Phys J, **47(**9), 893 (2004)
[39] Wenyi Yan, Qingping Sun, Xi-Qiao Feng, Linmao Qian, Int J Solids Struct, **44**, 1 (2007)

* Corresponding author: lgbujor@tuiasi.ro